

2019

# A Study of the Kratom Alkaloids and Their Binding to the $\mu$ -Opioid Receptor

Reba Elizabeth Ann Chamblee

University of Mississippi, rechambl@go.olemiss.edu

Follow this and additional works at: [https://egrove.olemiss.edu/hon\\_thesis](https://egrove.olemiss.edu/hon_thesis)



Part of the [Forensic Science and Technology Commons](#)

---

## Recommended Citation

Chamblee, Reba Elizabeth Ann, "A Study of the Kratom Alkaloids and Their Binding to the  $\mu$ -Opioid Receptor" (2019). *Honors Theses*. 1147.

[https://egrove.olemiss.edu/hon\\_thesis/1147](https://egrove.olemiss.edu/hon_thesis/1147)

This Undergraduate Thesis is brought to you for free and open access by the Honors College (Sally McDonnell Barksdale Honors College) at eGrove. It has been accepted for inclusion in Honors Theses by an authorized administrator of eGrove. For more information, please contact [egrove@olemiss.edu](mailto:egrove@olemiss.edu).

A STUDY OF THE KRATOM ALKALOIDS AND THEIR BINDING TO THE  $\mu$ -  
OPIOID RECEPTOR

By  
Reba Elizabeth Ann Chamblee

A thesis submitted to the faculty of The University of Mississippi in partial fulfillment of  
the requirements of the Sally McDonnell Barksdale Honors College.

Oxford  
May 2019

Approved By

---

Advisor: Dr. Murrell Godfrey

---

Advisor: Dr. Robert J. Doerksen

---

Reader: Dr. Susan Pedigo

© 2019  
Reba Elizabeth Ann Chamblee  
ALL RIGHTS RESERVED

## **ACKNOWLEDGEMENTS**

This project would not have been possible without the guidance of Dr. Murrell Godfrey, Caroline Spencer and the assistance of Dr. Robert Doerksen and Dr. Pankaj Pandey. I'd like to give a special thank you to Dr. Robert J. Doerksen and Dr. Susan Pedigo for serving on my thesis committee. I would also like to thank Marissa Teske for all her help throughout the entirety of this project. Her own research on fentanyl and its analogs inspired the perseverance of my own. Lastly, I want to give an acknowledgement to the Sally McDonnell Barksdale Honors College for whom gave me the opportunity to work on this thesis and develop my research skills.

Supercomputer support is acknowledged from NSF MRI 1338056 and the Mississippi Center for Supercomputer Research. Its contents are solely the responsibility of the authors and do not necessarily represent the official view of NIGMS or NIH or NSF. This investigation was conducted in part in a facility constructed with support from the Research Facilities Improvements Program (C06RR14503) from the National Institutes of Health (NIH) National Center for Research Resources.

## **ABSTRACT**

Reba Chamblee: A Study of the Kratom Alkaloids and Their Binding to the  $\mu$ -Opioid Receptor  
(Under the direction of Dr. Murrell Godfrey)

Kratom, a plant commonly found in southeast Asia, has traditionally been used for medicinal treatments. Recently, however, the popularity of the drug has significantly increased due to its euphoric effects, leading to it being used as an alternative to illegal opioids. Several alkaloid compounds have been isolated from the leaves of the plant. The main alkaloids seen are the following five alkaloids: mitragynine, 7-hydroxymitragynine, speciociliatine, speciogynine, and paynantheine. Two alkaloids, mitragynine and 7-hydroxymitragynine, have exhibited high potencies and are potentially even more potent than morphine. Previous studies have indicated that the main mediator of the psychoactive effects is the opioid receptor system, specifically the  $\mu$ -,  $\kappa$ -, and  $\delta$ - opioid receptors. The highest binding affinities occur at the  $\mu$ -opioid receptor and lesser affinities at the  $\kappa$ - and  $\delta$ - opioid receptors. In this study, the  $\mu$ -opioid receptor model was used to establish the ligand-receptor interactions between the receptors and the constituents of specific kratom alkaloids. This was accomplished using Schrodinger's Maestro molecular modeling software. The major natural alkaloids of the plant were selected for his study because of their high abundances within the kratom plant as well as their binding affinities. Docking of the ligands to the receptor took place after both the alkaloid ligands and the opioid receptor model were prepped for docking and a grid of the

active sites were generated. Data generated from each docking yielded information on the best poses/positions of the alkaloids for binding to the receptor, interactions between the ligands and receptors, and the estimated binding affinities. The study aimed to find patterns within the alkaloid structural group that would lead to the identification of key structural components and/or protein residues that are essential to binding with the  $\mu$ -opioid receptor. The results of this study will lead to a new understanding of the effects kratom and its alkaloids have within the human body and help determine its potential for abuse. In addition to the results found in this study, future studies will help create a database of these alkaloids and their structures to facilitate the process of identifying them and perceiving their interactions with the  $\mu$ -opioid receptor.

## TABLE OF CONTENTS

List of Figures and Tables.....	vi
Introduction.....	1
Materials and Methods.....	8
Results and Discussion.....	14
Conclusion.....	31
References.....	35
Appendix.....	38

## LIST OF FIGURES AND TABLES

Figure 1	Structures of alkaloids found in the kratom plant chosen for this study... 9
Figure 2	Structures of the opioid and opiate ligands chosen for this study .... 10
Figure 3	The three-dimensional structure of the $\mu$ - opioid receptor model 5C1M used in this study (11) ..... 11
Table 1	The interactions, docking scores, calculated MM-GBSA values, and $K_i$ values for each of the alkaloids. .... 15
Figure 4	The number of residues interacting in the binding pocket of each alkaloid ..... 16
Table 2	List of the specific hydrophobic residues seen in the binding pocket of mitragynine and 7-hydroxymitragynine. .... 20
Table 3	List of the specific hydrophobic residues seen in the binding pocket of mitragynine and 7-hydroxymitragynine ..... 20
Figure 5	The ligand-receptor interaction diagrams for mitragynine (left) and 7-hydroxymitragynine (right) ..... 21
Table 4	List of all the opioids, opiates, and alkaloids with their interactions and docking scores. .... 23
Figure 6	The number of residues interacting in the binding pocket of all the opioids and opiates ..... 24
Table 5	The MM-GBSA and $K_i$ values for all of the ligands..... 25



Table 6	Hydrophobic interaction residues seen in the binding pockets of mitragynine, 7-hydroxymitragynine, carfentanil, and fentanyl.....	27
Table 7	Polar interaction residues seen in the binding pockets of mitragynine, 7-hydroxymitragynine, carfentanil, and fentanyl .....	27
Figure 7	The number of interacting residues in the binding pocket for mitragynine, 7-hydroxymitragynine, carfentanil, and fentanyl. ....	28
Table 8	Comparison of the differences in docking score and MM-GBSA values between the three buprenorphine structures downloaded from the ChemSpider, PubChem, and Guide to Pharmacology websites .....	30
Figure A-1	Ligand-receptor interaction diagram for buprenorphine .....	38
Figure A-2	Ligand-receptor interaction diagram for carfentanil .....	38
Figure A-3	Ligand-receptor interaction diagram for corynantheidine.....	39
Figure A-4	Ligand-receptor interaction diagram for fentanyl .....	39
Figure A-5	Ligand-receptor interaction diagram for heroin .....	40
Figure A-6	Ligand-receptor interaction diagram for hydromorphone .....	40
Figure A-7	Ligand-receptor interaction diagram for lofentanyl .....	41
Figure A-8	Ligand-receptor interaction diagram for methadone .....	41
Figure A-9	Ligand-receptor interaction diagram for mitragynine pseudoindoxyl .....	42
Figure A-10	Ligand-receptor interaction diagram for morphine .....	42
Figure A-11	Ligand-receptor interaction diagram for o-desmethylnaloxone .....	43

Figure A-12	Ligand-receptor interaction diagram for oxycodone .....	43
Figure A-13	Ligand-receptor interaction diagram for paynantheine .....	44
Figure A-14	Ligand-receptor interaction diagram for speciociliatine .....	44
Figure A-15	Ligand-receptor interaction diagram for speciogynine .....	45
Figure A-16	Ligand-receptor interaction diagram for tramadol .....	45

## **Introduction:**

*Mitragyna speciosa*, also known as kratom, is a plant of the Rubiaceae (coffee) family indigenous to the countries of Thailand and Malaysia (1). Primarily the plant grows within the tropical and subtropical regions of Africa and southeast Asia. Most kratom trees grow to a height of 4 to 9 m with dark, glossy green leaves and deep yellow flowers. Based upon the color of the leaf vein, two types of kratom can be identified (2). Out of the two colors, red and green, red is usually preferred due to its characteristic bitterness and longer lasting effects. The leaves and smaller stems of the tree are mainly used for consumption. Fresh leaves, normally about 10 to 30 per day, are chewed and swallowed to obtain the desired effects, but they can also be dried for smoking, used for making tea, or ground into a powder to turn into a pill.

According to early documentation, kratom was first used in southeast Asia as an affordable, alternative to opium in the 1800s (3). However, it soon became traditional for the leaves and extracts of kratom to be used for medicinal treatments of mild problems, such as fever, cough, diarrhea, pain, and hypertension. Manual laborers have even used kratom for its stimulant effects as a way of combating strain, stress, and fatigue thereby enhancing their physical endurance, much like others have done with cocaine. Overtime, though, it also became known and used to subdue the symptoms associated with opiate withdrawal, given the affordability and availability (2). Recent reports have suggested that younger consumers of kratom are now using it as the base for a cocktail consisting of kratom tea, cough syrup, Coca-Cola, and ice cubes. This occurrence has become a source of concern since the consumers are now including additives, such as benzodiazepines,

with kratom to enhance its effects. The enhanced form of kratom has now become popular in the West, including the United States.

As for traditional uses in the West, kratom has become a source of managing pain due to its analgesic properties (3). Often, kratom is marketed as an herbal dietary supplement safe to treat chronic pain. It soon became an affordable alternative form of treating prescription opioid withdrawal as it did in southeast Asia. In Germany, there was also a single case of kratom being used to self-manage the withdrawal symptoms of alcohol. More recently, the euphoric effects of kratom has increased its popularity therefore leading to its popularization as a safe herbal product efficient at “giving a ‘legal’ high and as an alternative to other sedative and stimulant type drugs”.

Combinations of kratom and other substances have also become an increasingly prominent item to be sold via the internet, promising a more powerful high. For example, one concoction called ‘krypton’ combines powdered kratom leaves with o-desmethyltramadol, which was linked to nine cases of death in less than one year due to overdose. Therefore, it has become clear that kratom is rapidly morphing into a recreational drug that is not only gaining popularity among the youth in Thailand but in the West as well.

As with most other drugs, kratom has its own wide variety of reported side effects. For those having consumed kratom after more than a year, the main side effects include loss of weight, dehydration, constipation, and hyperpigmentation (3). Those users who used for longer periods also reported lethargy and tiredness. Based upon reports from an internet site, negative side effects also include the following: stomach aches, nausea, dizziness, vomiting, itchiness, unsteadiness, alternation between chills and

sweats, numbness in the mouth and throat, visual alterations, and sedation. According to an online survey in the United States, the primary negative effects of kratom use are primarily gastrointestinal related, such as nausea and constipation (4). The most frequent negative side effects reported were dizziness or drowsiness, constipation, and nausea, and with the exception of diarrhea, all negative effects appeared to be dose-dependent. Higher doses and more frequent dosing lead to higher odds of negative effects. Case reports from Western countries even suggest evidence of seizure and coma from ingestion of kratom.

Many positive effects of kratom have been reported in addition to the negative. According to experiences reported by kratom users on an internet site, positive side effects include a warm and tingly feeling, a sense of wellbeing, sensory enhancement, relaxation, analgesia, enhanced sociability, euphoria, and more energy (3). From a U.S. 2016 online survey, the most beneficial effects of kratom reported by users were less depressive mood, increased energy, and decreased pain (4). A dose-dependent effect was observed for the effects of increased energy, elevated mood, less depressive and anxious mood, and reducing or stopping opioid pain-relieving medication use. For effective reduction or discontinuation of opioid pain medication, the threshold dose per reported kratom use was 5 or more grams.

Kratom's tendency to act as both a stimulant and a sedative is dose dependent (3). Stimulant effects are experienced at lower doses while sedative effects are seen at higher doses. Regular users of kratom, however, are highly prone to developing a tolerance for the substance which often leads to increases in intake over time and possibly addiction. Results from a Malaysian study indicated that more than half of regular kratom users

ended up developing a severe dependence on the substance. Given the growing number of internet sites for purchasing kratom, addiction to kratom is likely to increase.

A variety of unpleasant physical and psychological symptoms can arise from the ceasing of kratom use. Physical symptoms include diarrhea, lethargy, joint pain, irritability, cramps, runny nose, and muscular pain (3). Intense craving, restlessness, hallucination, tension, delusion, aggression, nervousness, and sadness were all reported psychological symptoms. There were also reports of sleeplessness, moodiness, annoyance, depression, and feelings of anxiety. In several cases, long-term users of kratom had difficulty in giving it up. However, some reports show that while kratom withdrawal symptoms are aggravating, they were not as painful as those of opiate withdrawal. Withdrawal symptoms also usually disappear 1 to 3 days after cessation of use.

To date, more than 40 alkaloids have been isolated and chemically characterized from the kratom plant, with mitragynine being the main constituent and most abundant at 66% of the total alkaloid content (1,2). Mitragynine is also exclusive only to *Mitragyna speciosa*. In addition, several analogues of mitragynine (which include speciogynine, speciociliatine, and paynantheine) have been found to be major indole alkaloids present in the leaves of the plant (1). Another important but minor constituent is 7-hydroxymitragynine, with roughly 2% of the total alkaloid content. Most, if not all, of these alkaloids were able to be extracted using methanol or ethyl acetate. The relative amount of each alkaloid varies by geographic origin of the plant and season.

The mechanism of binding for the kratom alkaloids has been studied and most of the studies have indicated that the cause of the psychoactive effects is the opioid receptor

system (5). The alkaloids mitragynine and 7-hydroxymitragynine have displayed the highest binding affinities for the  $\mu$ -opioid receptor. At the human opioid receptors, mitragynine shows partial agonistic activity at the  $\mu$ -opioid receptor. It also illustrates activities at the  $\kappa$ - and  $\delta$ -opioid receptors but at lower potencies. The oxidized analogue 7-hydroxymitragynine was found to be a potent, partial agonist at the  $\mu$ -opioid receptor and showed some activity at both the  $\kappa$  - and  $\delta$ -opioid receptors. Other major natural alkaloids of kratom, including paynantheine, speciogynine, and speciociliatine, show agonist activities at the opioid receptors. To further confirm the opioid activities of these alkaloids, radio-ligand binding studies were performed. The binding of the functional assays was able to confirm the previously stated agonist and antagonist activities.

Previous studies done to figure out the binding of the alkaloids has come from animal cell/membrane receptor studies and computational studies (5). From these studies, binding affinities for the opioid receptors were able to be calculated, which suggested that mitragynine and 7-hydroxymitragynine had higher affinities than other alkaloids. To date there has only been one computational study found in the literature involving kratom. This study docked mitragynine and several analogues into the X-ray crystal structure of the  $\mu$ -opioid receptor (5). The X-ray crystal structure used in this study contained the bound morphinan-derived agonist BU72. The authors saw many similarities between the alkaloid (-)-mitragynine and the BU72 agonist, but also found important differences between their binding to the  $\mu$ -opioid receptor. BU72 and (-)-mitragynine both exhibit polar interactions between the protonated amines and the receptor. This is a known as an important binding of classic opioid agonists and antagonists. However, for mitragynine, the methoxyindole group is directed toward a different hydrophobic pocket when

compared to BU72. This difference causes changes to the hydrogen bonding taking place within the binding pocket. The enol ether group of the mitragynine is directed into the same hydrophobic region as BU72 that is involved in the hydrogen bonding network of another portion of the  $\mu$ -opioid receptor. If this functional group is removed a loss of activity can occur since no hydrogen bonding network is being formed (5). Another structural group examined in this study was the ethyl group on ring D of (-)-mitragynine. Similarly, to the enol ether group, the removal of the ethyl group would be expected to weaken the hydrophobic-ligand interactions and therefore reducing the binding activity. The predicted low-energy docking pose of the 7-hydroxymitragynine analogue was similar to that of (-)-mitragynine, but interestingly the 7-position hydroxy group does not seem to come in close contact with the receptor surface, meaning that potential hydrogen bonding does not help in the increasing potency afforded by the oxidation. Instead, it seems that slight bending introduced in the core of 7-hydroxymitragynine by modification is more important. The other major alkaloids and some derivatives were also computationally docked, which confirmed earlier antagonist activities and illustrated how its binding orientation weakened the activities. More studies on the binding of kratom are currently in progress and will hopefully bring about a fuller picture on the true human mechanistic receptor binding.

Many countries around the world, including Thailand, Malaysia, and Australia, have banned kratom due to its view as an addictive psychotropic plant; however, the United States does not currently have kratom as a federally controlled substance. In 2014, the US Food and Drug Administration (FDA) released a statement warning of the dangers of kratom and began seizing many kratom-containing shipments based on



consumer safety concerns (7). Due to concerns, several states have placed kratom and its alkaloids mitragynine and 7-hydroxymitragynine on the list of controlled substances. Since 2012, the US Drug Enforcement Administration (DEA) has had kratom listed as a “drug of concern”. The DEA, however, attempted to emergency schedule the main alkaloids of kratom, and therefore the plant itself, into federal Schedule I in August 2016. However, due to the significant public backlash faced by the DEA, they withdrew the intent in October 2016, and it has remained unscheduled since. The reason for the intended emergency scheduling revolved around a report issued by the Centers for Disease Control and Prevention (CDC) describing a large increase in calls to poison control centers entailing kratom between 2010 and 2015. According to the report, “the number of calls increased by tenfold from 26 in 2010 to 263 in 2015” (8). Out of the reported exposures, 7.4% were medically considered as major exposures, exhibiting life-threatening signs or symptoms and with some residual disability. Only one report was given of a single death in a person who was exposed to kratom as well as the medications lamotrigine and paroxetine.

Recently, however, the CDC has issued a new report, detailing new exposure data that includes unintentional drug overdose deaths involving kratom. Between 2011 and 2017, the national poison center received 1,807 calls concerning exposure to kratom (10). Analyzing data from the State Unintentional Drug Overdose Reporting System (SUDORS), the CDC determined that of the 27,338 overdose deaths occurring between July 2016 and December 2017, 152 (0.56%) of the decedents tested positive for kratom on postmortem toxicology. Of the 152 kratom-positive decedents, kratom was determined to be a cause of death for 91 of the cases. For seven deaths, kratom was the only

substance that tested positive on the postmortem toxicology; however, additional substances could not be ruled out as being present.

Kratom has been gaining interest as a potential non-addictive, alternative treatment for opioid withdrawal. However, there have not been many studies to back up this claim, and with continued rise in kratom use more and more concern has risen over its potential addictive properties instead. Its traditional medicinal uses have given way to abuse of the substance as a way of getting a high, and the growing availability of kratom via the internet and pop-up stores has led to the likelihood of a new generation of addicts among the American population. Therefore, more research into kratom's mechanism of binding with target receptors is vital to understanding the pharmacology and effects of the plant and its alkaloids as well as its potential for abuse. In this study, the ligand-receptor interactions of specific kratom alkaloids with the mu-opioid receptor in order to gain a better understanding of the influence specific structural characteristics have on the binding and pharmacology of these substances.

## **Materials & Methods:**

### **Ligand Selection**

All ligands chosen for computation docking to the active  $\mu$ -opioid receptor were chosen due to all having shown previous agonistic binding to the  $\mu$ -opioid receptor. The kratom alkaloids chosen include mitragynine, 7-hydroxymitragynine, paynantheine, speciociliatine, speciogynine, corynantheidine, and mitragynine pseudoindoxyl (see Figure 1). All other ligands chosen for this study are considered opioids or opiates and include fentanyl, carfentanil, lofentanil, tramadol, o-desmethyltramadol, oxycodone,

methadone, buprenorphine, hydromorphone, morphine, and heroin (see Figure 2). The main software used for the computational binding was the Maestro Suite by Schrödinger which is a molecular modeling software (11).

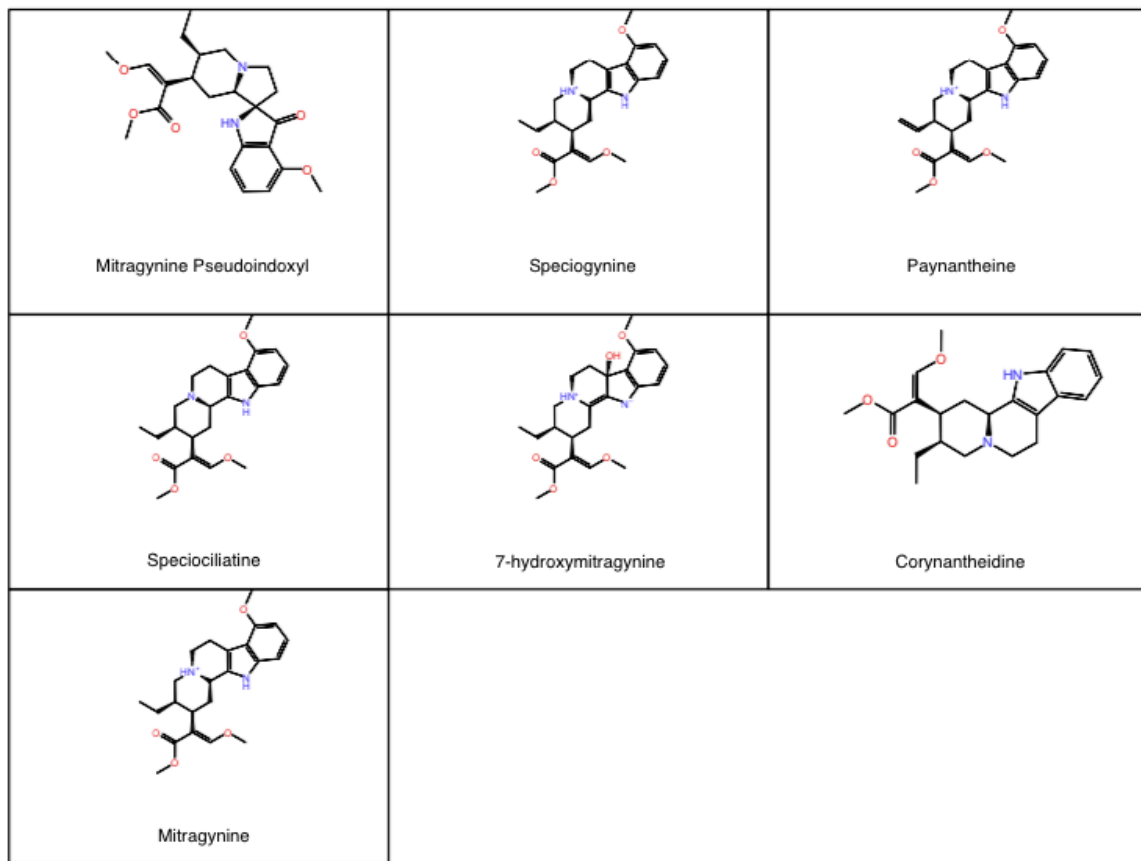


**Figure 1: Structures of alkaloids found in the kratom plant chosen for this study**

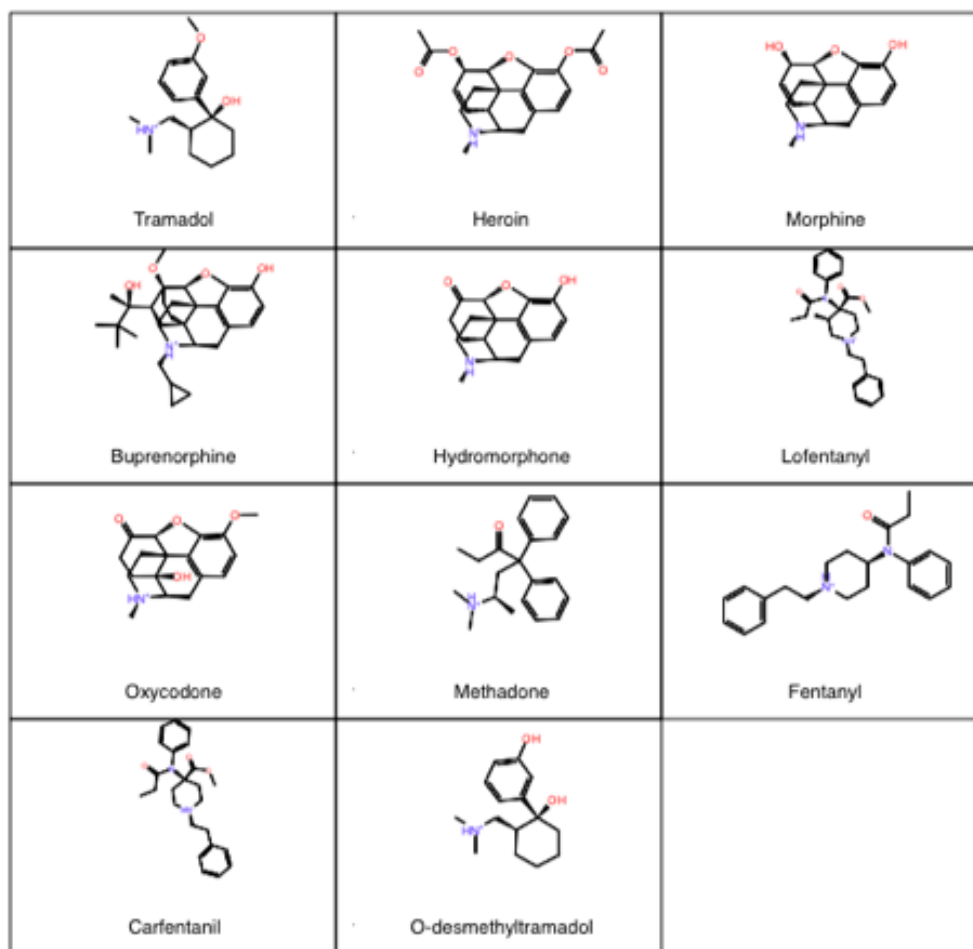


**Figure 2: Structures of the opioid and opiate ligands chosen for this study**

### Protein Selection and Preparation

As previously mentioned, the receptor chosen for the study was the  $\mu$ -opioid receptor (see Figure 3). The active-state  $\mu$ -opioid receptor crystal structure was solved by Huang et al. (12). The published crystallized model was imported into the Maestro software for prepping through its Protein Data Bank file, 5C1M. Using the Protein Preparation Wizard, any issues occurring within the protein structure, such as missing residues or hydrogens, misoriented structural groups, or incomplete side chains and

loops, were corrected for. Specific residues are essential to the binding of ligands to the  $\mu$ -opioid receptor and must be present in the binding pocket. These residues include ASP 147, TYR 148, HIS 54 and MET 151. The protein preparation process helped to ensure that the most accurate protein model was being used to dock each ligand. The protein model used in this study was prepared by Dr. Pankaj Pandey at the University of Mississippi.

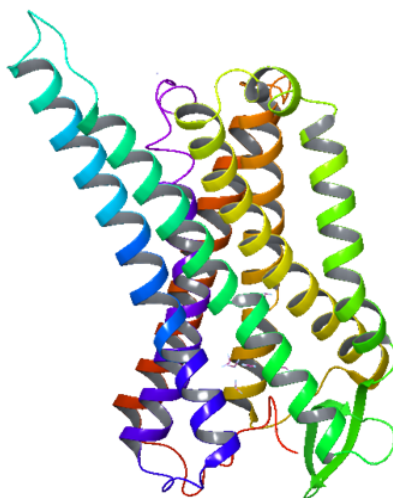


**Figure 3: The three-dimensional structure of the  $\mu$ -opioid receptor model 5C1M used in this study (12).**

### **Ligand Preparation**

All ligands were sketched in Maestro's 2D sketcher, available within the program's primary workspace, or imported from PubChem via the structure's SD file when available (13). Once the ligand structures were successfully entered into Maestro, the two-dimensional ligands were transformed into three-dimensional structures through the LigPrep protocol. LigPrep ensures that the ligand has been prepared for docking to

the receptor. Other than converting the structure to its three-dimensional form, the ligand preparation also included the following steps: addition of hydrogens, removal of unwanted molecules, neutralization of charged groups, generation of ionization states, generation of tautomers, filtering of structures, generation of alternative chiralities, generation of low-energy ring conformations, removal of problematic structures, and optimization of geometries. These steps are essential to preparing the ligand properly for the most accurate docking study performance.

### **Grid Generation**

The grid generation protocol was used after the preparation of both the protein and the ligands. Grid generation was used to prepare and determine the docking receptor grid of the  $\mu$ -opioid binding pocket. In order to determine where the binding pocket is located, the morphinan derivative BU72, which was bound in the binding pocket of the crystalline  $\mu$ -opioid receptor used in the study, was located. Since this derivative is bound to the receptor, the location of the compound indicates the area of the binding pocket. The grid was therefore formed around BU72, ensuring the correct location and space of the binding pocket for further ligand docking. By determining a grid around the binding pocket of the receptor, the ligands are able to dock more accurately to the receptor, which occurs during the glide docking.

### **Glide Docking**

Glide docking was the next step in the Maestro protocol. The process took the previously prepared ligands and docked them in the grid generated within the receptor

from the previous step. The ligands chosen were docked using the standard precision (SP) method. Constraints were not used on the present binding pocket residues of the receptor during the glide docking. Up to five possible poses were created for each ligand and subsequently docked to the receptor. The best, or most accurate, pose was found through the docking scores, GlideScores, and Glide Emodel scores generated during the glide docking. Looking at these scores in combination helps determine the best overall binding pose for the receptor. The GlideScore maximizes the separation of compounds with strong binding affinity from those that have little to no binding affinity (9). As an empirical scoring function, the value incorporates terms that take into account the physics of the binding process, which includes the following terms: hydrogen bond terms, lipophilic-lipophilic term, rotatable bond penalty, protein-ligand energy contributions, and hydrophobic enclosure. The calculated Glide Emodel score places more emphasis on the force field components of the binding, such as van der Waals and electrostatic energies. Glide Emodel scores compare and rank poses of the same ligand to determine the most likely pose of said ligand. After the glide docking, ligand interaction diagrams were produced for every pose of each ligand. The two-dimensional ligand interaction diagrams show a view of the binding pocket of the receptor with the ligand bound as well as the specific residues that are interacting with the ligand. Each type of ligand - receptor interaction in the binding pocket is also illustrated through color-coding of the residues. These interactions, hydrogen bonding and  $\pi$ - $\pi$  stacking for example, are even measurable in angstroms using the ligand interaction diagrams. The best pose interaction diagrams of each specific ligand were thoroughly analyzed and compared to seek trends in structural characteristics and residue interactions.

## **Calculations**

After all ligands have been docked, multiple calculations can be executed within the Maestro software. For this project, the main focus was on the binding free energy estimations. The method used is known as the Prime Molecular Mechanics/Generalized Born Surface Area (prime MM-GBSA), which can estimate the relative binding affinities for the ligands. While the values will not be consistent with those of experimental binding affinities, the calculation can be used to rank the relative binding affinities of the ligands which should be comparable to the experimental values rankings (11).

## **Results & Discussion:**

Following the successful docking of all ligands, the best, most favorable pose was chosen for each based upon their GlideScore and Glide Emodel values. The more negative values indicated better binding, so the best pose chosen was based upon the most negative GlideScore and Glide Emodel value. Once these had been chosen, the ligand-receptor interaction diagrams for each were used to make comparisons between the alkaloids and the many opioids. These diagrams were analyzed at 5 angstroms. The top poses for each ligand were also used to calculate their MM-GBSA values.

## **Kratom Alkaloids**

Based upon the ligand interaction diagrams, all the kratom alkaloids interact in some form with either HIS 54 or ASP 147 (see Table 1). These two residues in addition to MET 151 and TYR 148 are vital for binding to the  $\mu$ -opioid receptor and are seen in



the binding pocket of all those that bind. Almost every alkaloid interacts through hydrogen bonding with ASP 147, with the exceptions of 7-hydroxymitragynine and speciogynine. Mitragynine is the only alkaloid to interact with both residues. However, ASP 147 is at least present in the binding pockets of all the alkaloids even if there is no direct interaction between the molecule and the receptor. The same can be applied to HIS 54 as well. Notably, there are no salt-bridge or  $\pi$ - $\pi$  stacking interactions for any of the alkaloids.

**Table 1: The interactions, docking scores, calculated MM-GBSA values, and  $K_i$  values for each of the alkaloids. The alkaloids are listed from most negative to most positive docking score.**

<b>Ligand</b>	<b><math>\pi</math>-cation</b>	<b>Hydrogen bond</b>	<b>Docking Score</b>	<b>MM-GBSA Value (kcal/mol)</b>	<b><math>K_i</math> Value (<math>\mu</math>M) [5,14]</b>
Mitragynine	HIS 54	ASP 147	-7.151	-50.24	$0.230 \pm 0.048$
Corynantheidine	-	ASP 147	-6.927	-43.77	-
7-hydroxymitragynine	HIS 54	H <sub>2</sub> O	-6.658	-36.28	$0.037 \pm 0.004$
Speciociliatine	-	ASP 147	-5.987	-24.98	$0.560 \pm 0.168$
Paynantheine	HIS 54	HIS 54	-5.871	-26.2	$0.410 \pm 0.152$
Speciogynine	HIS 54	-	-5.542	-19.77	$0.728 \pm 0.061$
Mitragynine Pseudoindoxyl	-	ASP 147, H <sub>2</sub> O	-3.893	-22.23	$0.0008 \pm 0.0002$

Both corynantheidine and speciociliatine have the same hydrogen bonding interaction with ASP 147. They also have equal numbers of hydrophobic, polar, and negatively charged residues within their binding pockets. However, they do not have the same number of positively charged residues. Corynantheidine has one positively charged residue, LYS 233, while speciociliatine does not contain any. Speciociliatine also has a GLY 325 residue within its binding pocket, and corynantheidine does not. These couple of differences could possibly explain the difference in their docking scores.

When it comes to residue interactions in the binding pockets, the alkaloids have similar numbers of residues (see Figure 4). Corynantheidine and 7-hydroxymitragynine

even contain equivalent numbers of all the residue types. Both of them also occur next to each other in the docking score rankings of the alkaloids, which could be due to these equivalent numbers. Speciociatine has the same number of hydrophobic, polar, and negatively charged residues as corynantheidine and 7-hydroxymitragynine as well but does not have a positively charged residue like the other two. This lack of a positively charged residue could be why it has a more positive docking score and why there's a wider gap in docking score value.

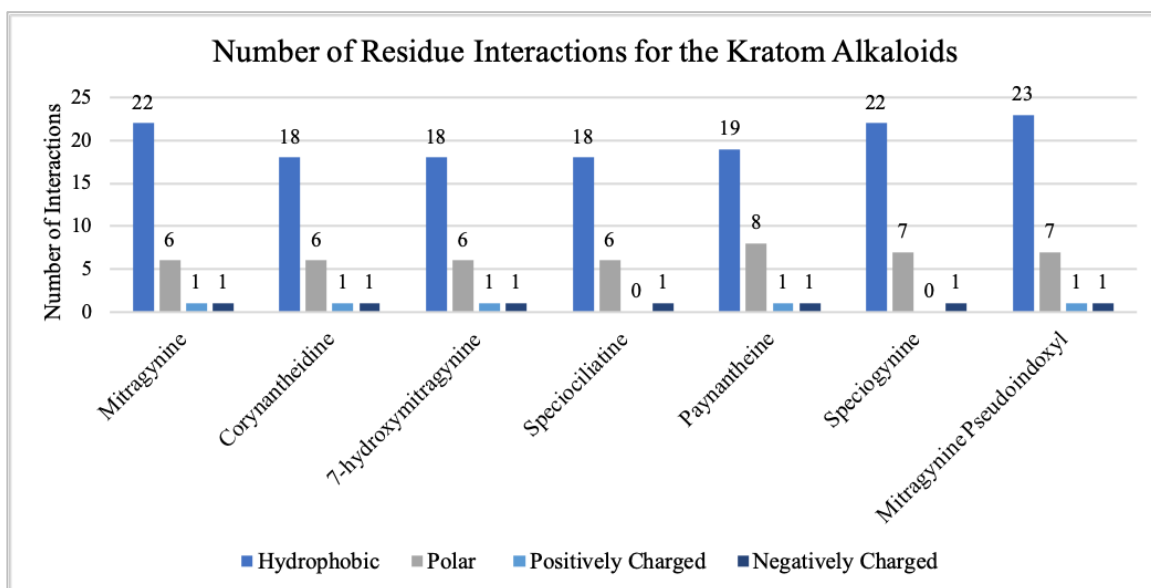


**Figure 4: The number of residues interacting in the binding pocket of each alkaloid**

Mitragynine and speciogynine share the same number of hydrophobic and negatively charged residues but have docking scores further apart, -7.151 and -5.542 respectively. However, mitragynine has a positively charged residue that is not seen in the binding pocket of speciogynine. Speciogynine also has one more polar residue than

mitragynine. These factors could lead to the difference in docking score. The direct receptor interactions could pertain to mitragynine and speciogynine's difference in GlideScore as well. Both have a  $\pi$ -cation bond with HIS 54; however, mitragynine has an extra interaction, a hydrogen bond with ASP 147.

While mitragynine has the most negative docking score, mitragynine pseudoindoxyl has the worst, or least negative, docking score out of all the alkaloids at -3.893. The pseudoindoxyl form contains one more hydrophobic and one more polar residue than mitragynine, but they both contain the same two positively and negatively charged residues, ASP 147 and LYS 233. They also share a hydrogen bond with ASP 147. However, their other direct receptor interactions differ. As previously stated, mitragynine has a  $\pi$ -cation bond with HIS 54. Mitragynine pseudoindoxyl has a hydrogen bond with water in addition to its bond with ASP 147. This water molecule also interacts with the oxygen of a carbonyl group on the structure.

After reviewing the ligand-receptor interaction diagrams for each alkaloid, paying attention to the specific polar residues within the binding pocket, it can be seen that all the alkaloids have at least 5 polar residues in common. All contain HIS 54, SER 55, ASN 127, GLN 124, and HIE 297. HIE is a histidine residue that has a hydrogen on the epsilon nitrogen. A sixth polar residue, THR 120, is shared by all the alkaloids except for paynantheine and speciogynine. In the place of THR 120, paynantheine has the polar residues THR 218 and HIE 319 while speciogynine has SER 125 and HIE 319. Mitragynine pseudoindoxyl has the added polar residue SER 53 in addition to the other six previously mentioned.

For binding affinities, the ranking of the alkaloids by the binding free energy estimations is very similar to their experimental binding affinity rankings. Mitragynine exhibits the most negative MM-GBSA value out of all the alkaloids and also has a smaller binding affinity value, suggesting a tighter binding with the  $\mu$ -opioid receptor. Speciociliatine, speciogynine, and paynantheine all have similar binding affinity values as well as similar MM-GBSA values, ranging from -26.2 to -19.77 kcal/mol. However, the MM-GBSA value for 7-hydroxymitragynine does not match ranking wise with its binding affinity found in the literature nor does mitragynine pseudoindoxyl. A binding affinity ( $K_i$ ) value could not be found for corynantheidine.

### **Mitragynine and 7-hydroxymitragynine**

Much of the literature on these two alkaloids has stated that 7-hydroxymitragynine is the most potent alkaloid, with its potency just slightly higher than that of mitragynine. However, much of the data in this project seems to point at the opposing idea. Mitragynine has consistently had a more negative docking score compared to 7-hydroxymitragynine. The calculated MM-GBSA values even suggest that mitragynine has a higher affinity for the  $\mu$ -opioid receptor than 7-hydroxymitragynine. Several different MM-GBSA sampling methods were used to see if the number could become even more negative. These sampling methods included minimization with and without constraints, minimization of side chains with and without constraints, and minimization of polar hydrogens with and without constraints. It stayed consistently around -36 kcal/mol throughout each calculation.

When comparing the ligand interaction diagrams between mitragynine and 7-hydroxymitragynine, the former contains more hydrophobic residues than the later (see Figure 4). Seventeen of the hydrophobic residues seen in the 7-hydroxymitragynine pocket are shared with mitragynine, which includes TRP 133, TYR 128, CYS 217, CYS 140, PHE 123, VAL 143, ILE 144, TYR 148, MET 151, VAL 300, VAL 236, ILE 296, TYR 326, ALA 240, TRP 293, ILE 322, and TRP 318 (see Table 2). The eighteenth residue of 7-hydroxymitragynine is PHE 152. The five additional hydrophobic residues seen in the mitragynine pocket are TYR 75, ALA 117, CYS 321, ALA 323, and PHE 237. However, they both contain the same amount of polar, negatively, and positively charged residues. They both contain the same specific polar residues, which includes HIS 54, SER 55, ASN 127, GLN 124, THR 120, and HIE 297. The same can be said for the negatively and positively charged residues since they both have ASP 147 and LYS 233.

**Table 2: List of the specific hydrophobic residues seen in the binding pocket of mitragynine and 7-hydroxymitragynine. The green coloring represents all the residues that the two have in common.**

<b>Hydrophobic Residue</b>	<b>Mitragynine</b>	<b>7-hydroxymitragynine</b>
TRP 133	+	+
TYR 128	+	+
TYR 75	+	
CYS 140	+	+
CYS 217	+	+
PHE 123	+	+
VAL 143	+	+
ILE 144	+	+
ALA 117	+	
TYR 148	+	+
MET 151	+	+
VAL 300	+	+
VAL 236	+	+
PHE 237	+	
ILE 296	+	+
TYR 326	+	+
ALA 240	+	+
TRP 293	+	+
ALA 323	+	
ILE 322	+	+
CYS 321	+	
TRP 318	+	+
PHE 152		+
LEU 324		
LEU 219		

**Table 3: List of the specific polar residues seen in the binding pocket of mitragynine and 7-hydroxymitragynine. The green coloring represents all the residues that the two have in common.**

<b>Polar Residue</b>	<b>Mitragynine</b>	<b>7-hydroxymitragynine</b>
HIS 54	+	+
SER 55	+	+
ASN 127	+	+
GLN 124	+	+
THR 120	+	+
HIE 297	+	+

The direct interactions between the two differ as well. While they both share a  $\pi$ -cation bond with HIS 54, their other interactions are not equivalent. 7-hydroxymitragynine also has a water molecule interacting with a carbonyl oxygen and TYR 148 which is not seen for mitragynine (see Figure 5).

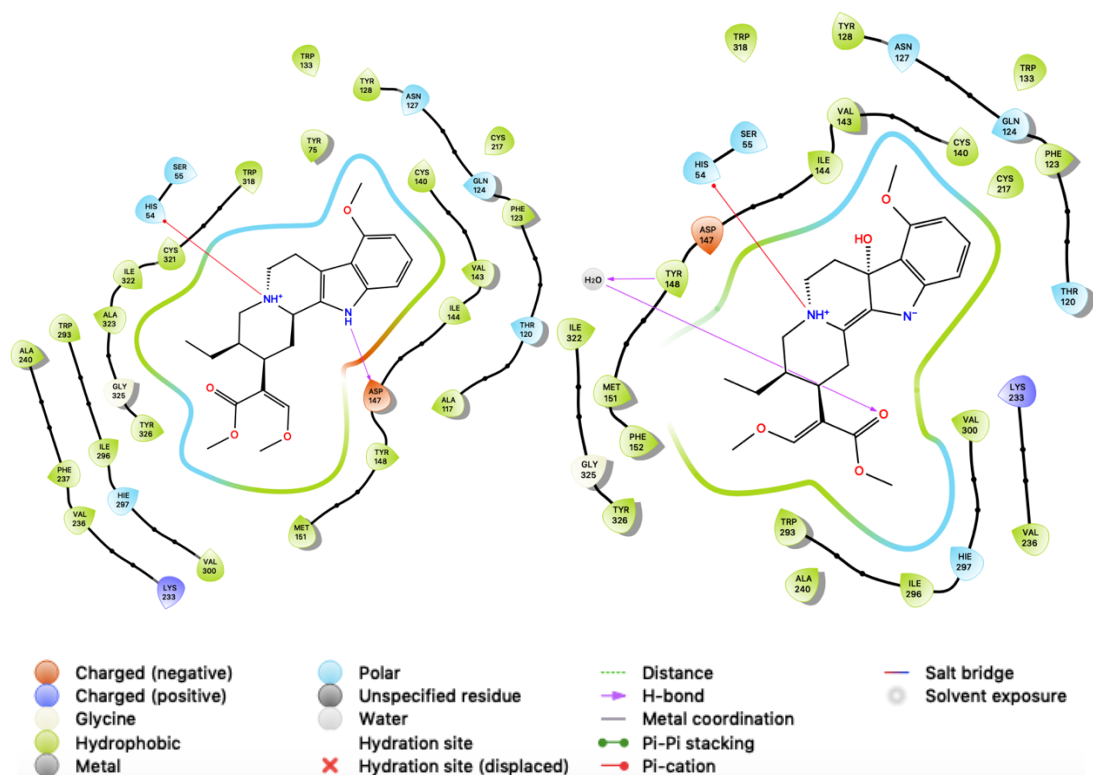


**Figure 5: The ligand-receptor interaction diagrams for mitragynine (left) and 7-hydroxymitragynine (right)**

## Comparison of Alkaloids to Opioids and Opiates

To better understand the fit of the kratom alkaloids within the sphere of psychoactive substances, the alkaloids were compared to other well-known opioids and opiates.

Looking at the ligand-receptor interactions brings about many commonalities and differences. When it comes to direct ligand-receptor interactions, salt bridges and  $\pi$ - $\pi$  stacking are only seen in the opioids and opiates, not the alkaloids (see Table 3). Every opioid and opiate has a salt-bridge with ASP 147 while the alkaloids do not, and the  $\pi$ - $\pi$  stacking only occurs for a few of the opioids/opiates, such as carfentanil, fentanyl, methadone, and hydromorphone. HIS 54 reacts through a  $\pi$ -cation bond with only the alkaloids while TYR 148 reacts through a  $\pi$ -cation bond with only the opioids/opiates. Only two of the chosen ligands, methadone and paynantheine, interacted through hydrogen bonding with HIS 54.



**Table 4: List of all the opioids, opiates, and alkaloids with their interactions and docking scores. All ligands are in order of most negative docking score to least negative. Each color represents ligands that have the same interactions with the same residues.**

Ligand	Salt-bridge	$\pi$ -cation	$\pi$ - $\pi$ stacking	Hydrogen bond	Docking Score
O-desmethyltramadol	ASP 147	TYR 148	-	ASP 147	-7.967
Carfentanil	ASP 147	-	TYR 326, TRP 293	ASP 147	-7.227
Mitragynine	-	HIS 54	-	ASP 147	-7.151
Corynantheidine	-	-	-	ASP 147	-6.927
Fentanyl	ASP 147	-	TYR 326, TRP 293	ASP 147	-6.833
7-hydroxymitragynine	-	HIS 54	-	H <sub>2</sub> O	-6.658
Methadone	ASP 147	-	TYR 326	HIS 54	-6.422
Oxycodone	ASP 147	TYR 148	-	ASP 147	-6.413
Lofentanyl	ASP 147	-	-	-	-6.142
Hydromorphone	ASP 147	TYR 148	HIE 297	H <sub>2</sub> O	-6.135
Buprenorphine	ASP 147	TYR 148	-	ASP 147, H <sub>2</sub> O	-6.116
Speciociliatine	-	-	-	ASP 147	-5.987
Morphine	ASP 147	TYR 148	-	-	-5.938
Paynantheine	-	HIS 54	-	HIS 54	-5.871
Heroin	ASP 147	-	-	ASP 147, LYS 303	-5.729
Tramadol	ASP 147	-	-	ASP 147	-5.633
Speciogynine	-	HIS 54	-	-	-5.542
Mitragynine Pseudoindoxyl	-	-	-	ASP 147, H <sub>2</sub> O	-3.893

Compared to the alkaloids, most of the opioids and opiates do not share similar numbers of hydrophobic, polar, positively, and negatively charged residues (see Figure 6). All the opioids and opiates have varying numbers of these residues, and the only ones of the opioid/opiate group to even share similarities within themselves are carfentanil and fentanyl. Hydrophobic residue counts range from 13 to 21 for the opioid/opiate group while those of the alkaloids range from 18 to 23. Two common hydrophobic residues seen for all of the chosen ligands were MET 151 and TYR 148, which are two residues essential for binding. The range for polar residues, however, is similar as the alkaloids range from 6 to 8 while the opioids range from 4 to 6 with the exception of buprenorphine which has 11 polar residues. Comparing the specific polar residues within the binding pockets of each ligand also reveals that all contain at least GLN 124, SER 55, HIS 54, and HIE 297 as polar residues. When it comes to positively charged residues, all

of the alkaloids, opioids, and opiates contain the positively charged LYS 233 residue except for speciogynine and speciociliatine. The negatively charged residue seen for all the ligands is ASP 147, which is another residue essential for binding to the  $\mu$ . Another residue, GLY 325, is seen in the binding pocket of every ligand with the exceptions of o-desmethyiltramadol, corynantheidine, and mitragynine pseudoindoxyl.

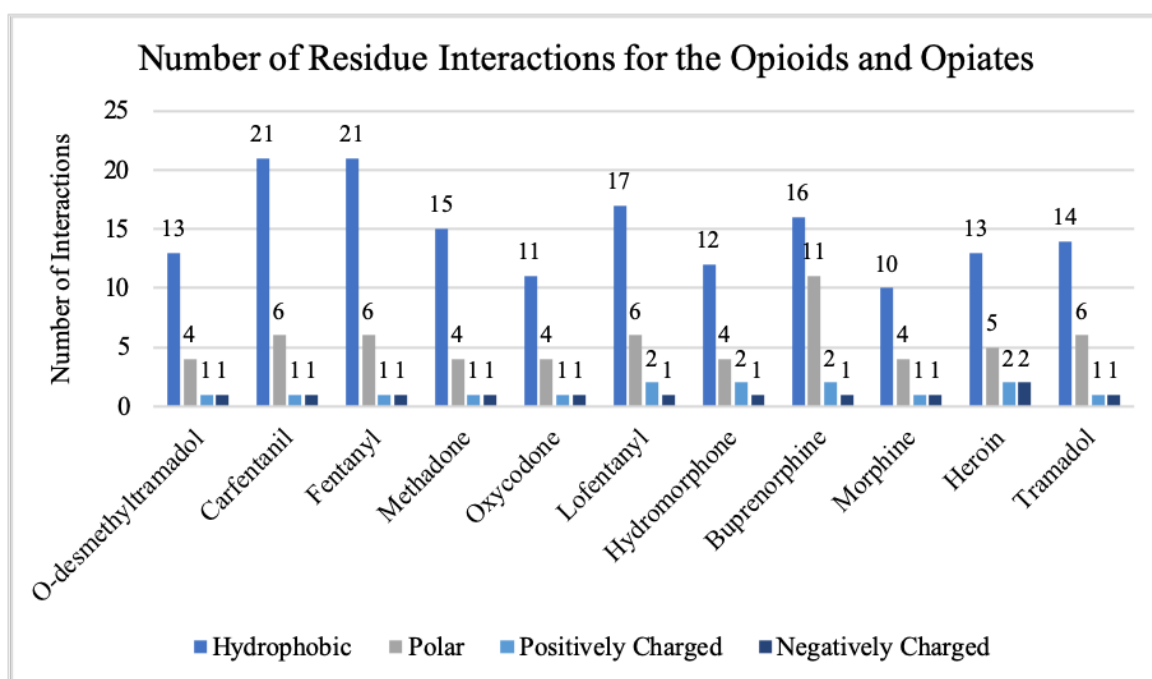


**Figure 6: The number of residues interacting in the binding pocket of all the opioids and opiates**

To further compare the binding of the alkaloids to the opioids/opiates, the calculated MM-GBSA values of all were compared to the known literature values for binding affinity to create a ranking of best to worst binding (see Table 4). The ranking of the alkaloids based upon MM-GBSA values, which was mentioned previously, is similar

to that of their  $K_i$  values. However, the order of the opioids based upon their MM-GBSA values is not very similar to their  $K_i$  value rankings, making it difficult to understand where the kratom alkaloids fits within the scheme of how they bind. Just looking at the MM-GBSA values, though, shows indications that at least the alkaloid mitragynine exhibits strong binding with the  $\mu$ -opioid receptor, and considering its placement in relation to carfentanil and fentanyl, this could mean that mitragynine is possibly a very potent alkaloid.

**Table 5: The MM-GBSA and  $K_i$  values for all of the ligands. Ligands are ordered from most negative to least negative MM-GBSA value. MM-GBSA values are in kcal/mol.**

<b><u>Compound</u></b>	<b><u>MM-GBSA Value (kcal/mol)</u></b>	<b><u><math>K_i</math> Values (nM) [5,14,15,16]</u></b>
Carfentanil	-61.46	$0.122 \pm 0.098$
Fentanyl	-54.15	$1.275 \pm 0.075$
Mitragynine	-50.24	$230 \pm 48$
Oxycodone	-48.89	$25.9$
Hydromorphone	-48.15	$0.365$
Morphine	-47.63	$0.74 \pm 0.4$
O-desmethyiltramadol	-47.58	$121.7 \pm 118.3$
Corynantheidine	-43.77	-
Methadone	-39.13	$3.38$
Heroin	-37.93	$360 \pm 130$
Lofentanyl	-36.89	$0.039 \pm 0.016$
7-hydroxymitragynine	-36.28	$37 \pm 4$
Tramadol	-33.2	$13,050 \pm 11,750$
Buprenorphine**	-32.15	$0.216$
Paynantheine	-26.2	$410 \pm 152$
Speciociliatine	-24.98	$560 \pm 168$
Mitragynine Pseudoindoxyl	-22.23	$0.8 \pm 0.2$
Speciogynine	-19.77	$728 \pm 61$
Buprenorphine*	$23.34$	$0.216$

\*Buprenorphine structure taken from the PubChem website.

\*\*Buprenorphine structure taken from the ChemSpider website.

## Mitragynine, 7-hydroxymitragynine vs. Carfentanil, Fentanyl

As carfentanil and fentanyl are a couple of the most well-known compounds for their potency and deadliness, a comparison between them and the two supposedly potent alkaloid mitragynine and 7-hydroxymitragynine was called for to see how they relate.

To begin with, their direct interactions with the  $\mu$ -opioid receptor both have similarities and differences. Carfentanil, fentanyl, and mitragynine all share a hydrogen bond with ASP 147. 7-hydroxymitragynine does not share a hydrogen bond with ASP 147. In fact, it does not directly interact with that residue at all, though it is in the binding pocket. Instead, 7-hydroxymitragynine and mitragynine share a  $\pi$ -cation bond with HIS 54. 7-hydroxymitragynine also has hydrogen bonding with a water molecule not seen in any of the other ligands. Carfentanil and fentanyl have salt-bridges with ASP 147 and  $\pi$ - $\pi$  stacking with TYR 326 and TRP 293 which is not seen in the two alkaloids.

One interesting finding is that all four of these ligands share very similar numbers of residue interactions. Carfentanil and fentanyl both have 21 hydrophobic residue interactions while mitragynine and 7-hydroxymitragynine have 22 and 18 respectively (see Table 5). All of the ligands have 6 polar residues, 1 positively charged residue, and 1 negatively charged residue. The positively and negatively charged residues happen to be ASP 147 and LYS 233 for all four ligands. Out of all the hydrophobic residues, fifteen of them are shared between all four ligands: TRP 133, CYS 140, CYS 217, VAL 143, ILE 144, TYR 148, MET 151, VAL 300, VAL 236, ILE 296, TYR 326, ALA 240, TRP 293, ILE 322, and TRP 318 (see Table ). For the polar residues, all four have the HIS 54, SER 55, THR 120, GLN 124, and HIE 297 residues. Mitragynine, 7-hydroxymitragynine, and

carfentanil all also share ASN 127 as a polar residue. The sixth polar residue for fentanyl is THR 218.

**Table 6: Hydrophobic interaction residues seen in the binding pockets of mitragynine, 7-hydroxymitragynine, carfentanil, and fentanyl. The blue coloring represents all of the residues the four ligands have in common**

<b>Hydrophobic Residue</b>	<b>Mitragynine</b>	<b>7-hydroxymitragynine</b>	<b>Carfentanil</b>	<b>Fentanyl</b>
TRP 133	+	+	+	+
TYR 128	+	+		
TYR 75	+			
CYS 140	+	+	+	+
CYS 217	+	+	+	+
PHE 123	+	+		+
VAL 143	+	+	+	+
ILE 144	+	+	+	+
ALA 117	+		+	+
TYR 148	+	+	+	+
MET 151	+	+	+	+
VAL 300	+	+	+	+
VAL 236	+	+	+	+
PHE 237	+		+	+
ILE 296	+	+	+	+
TYR 326	+	+	+	+
ALA 240	+	+	+	+
TRP 293	+	+	+	+
ALA 323	+		+	+
ILE 322	+	+	+	+
CYS 321	+		+	+
TRP 318	+	+	+	+
PHE 152		+		
LEU 324			+	+
LEU 219			+	

**Table 7: Polar interaction residues seen in the binding pockets of mitragynine, 7-hydroxymitragynine, carfentanil, and fentanyl. The blue coloring represents all of the residues the four ligands have in common**

<b>Polar Residue</b>	<b>Mitragynine</b>	<b>7-hydroxymitragynine</b>	<b>Carfentanil</b>	<b>Fentanyl</b>
HIS 54	+	+	+	+
SER 55	+	+	+	+
ASN 127	+	+	+	
GLN 124	+	+	+	+
THR 120	+	+	+	+
HIE 297	+	+	+	+
THR 218				+

The rankings of these four compounds based upon MM-GBSA values is similar to that of their binding affinities. The most negative MM-GBSA value is assigned to carfentanil with fentanyl, mitragynine, and 7-hydroxymitragynine following in that order (see Table 4). However, based upon the binding affinity ranges the order should be carfentanil, fentanyl, 7-hydroxymitragynine, then mitragynine. A possible explanation for the difference the two could be due to the fact that the best docking pose chosen for 7-hydroxymitragynine does not involve a direct interaction or bond with ASP 147 like the other three ligands have.

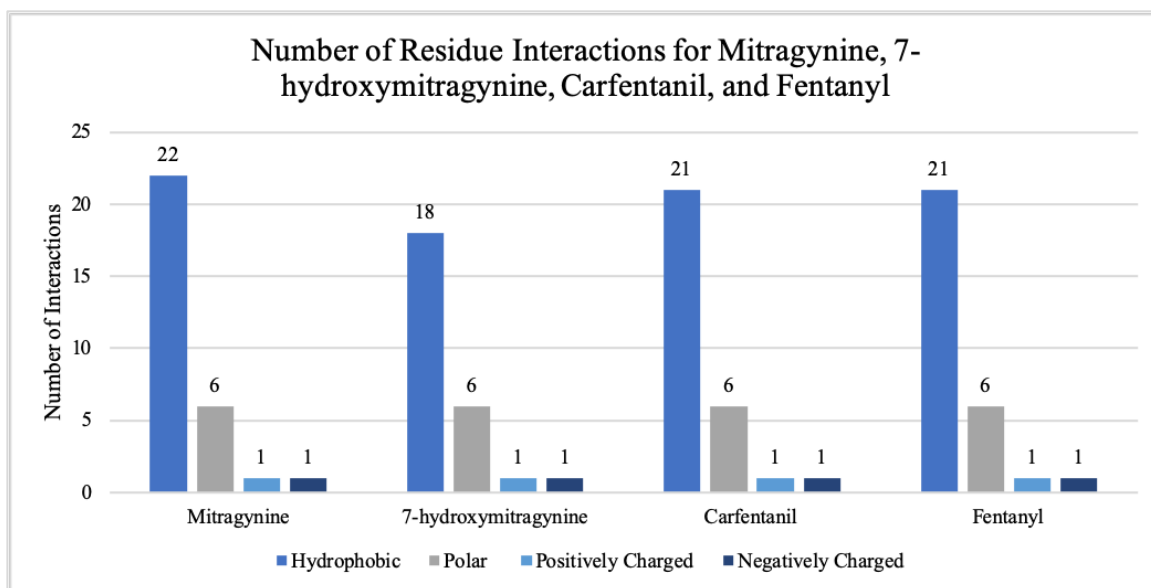


**Figure 7: The number of residues interacting in the binding pocket for mitragynine, 7-hydroxymitragynine, carfentanil, and fentanyl.**

## Buprenorphine

Over the course of docking ligands in this study and calculating the MM-GBSA values, an issue began to arise. Specifically, an issue involving the docking of buprenorphine. To begin with, the two-dimensional structure of buprenorphine was downloaded from the PubChem website then uploaded into Maestro. When trying to dock this structure, the glide docking failed, and it failed multiple times. Eventually, however, the structure was able to be docked to the receptor and gave the GlideScore and Glide Emodel values shown in the previous table, 23.49 kcal/mol. However, the problem really came to head when calculating the MM-GBSA value. If a ligand shows affinity for the receptor in Maestro, then the MM-GBSA value for the ligand should be a negative number. For buprenorphine, though, the value was positive when it should've been negative due to its partial agonistic activity at the  $\mu$ -opioid receptor. To try and combat this, the MM-GBSA value was calculated using various sampling methods, including minimization with and without constraints, minimization of side chains with and without constraints, and minimizations of polar hydrogens with and without constraints. None of these calculations ever caused the MM-GBSA value for buprenorphine to be anything other than positive. The next thought was that maybe the issue could be with the structure. Therefore, the structure was downloaded in both its two-dimensional and three-dimensional forms from PubChem and ChemSpider to see if there was a difference in values produced for each imported structure. The GlideScore and Glide Emodel values between each structure did not have a very large difference. However, once again, the MM-GBSA values were extremely different between each. The two-dimensional ChemSpider structure, though, did give a negative MM-GBSA value of -32.15 kcal/mol.

The three-dimensional structures were also ruled out as options due to the LigPrep function of the method. LigPrep is used to convert two-dimensional structures into three-dimensional structures ready for binding, so using this protocol on an already 3D structure could change parts of the structure that shouldn't be. To further see if the structures could be a part of the issue, a structure was downloaded from another site, the Guide to Pharmacology website, to compare with the versions from PubChem and ChemSpider. However, this third structure also gave a positive MM-GBSA value, one that was even more positive than the value from the PubChem structure (see Table 6). Therefore, it was concluded that the most likely reasons for the issue could be due to the differing file types for each structure, having corrupted files, or the program itself was not equipped to handle the complexity of the buprenorphine structure (see Figure 2).

**Table 8: Comparison of the differences in docking score and MM-GBSA values between the three buprenorphine structures downloaded from the ChemSpider, PubChem, and Guide to Pharmacology websites**

	<b><u>Docking Score</u></b>	<b><u>MM-GBSA Value (kcal/mol)</u></b>
Buprenorphine CS	-7.837	-32.15
Buprenorphine PC	-6.116	23.34
Buprenorphine GTP	-5.091	40.35



### **Conclusions:**

Kratom is a plant seen mainly in southeast Asian countries that has traditionally been used to treat people medically. Its side effects range all the way from dizziness to coma. However, it has been recently been gaining attention for its possible use as an alternative opioid withdrawal treatment. Several concerns have risen due to this attention about the potency of its alkaloids and whether it has more potential for abuse than for treatment, especially since there have been studies showing that users have become addicted to the substance over time. It has become extremely important to figure out and understand the interactions that kratom has within the body. The main way of interactions is said to be with opioid receptor system, specifically the  $\mu$ -,  $\kappa$ -, and  $\delta$ -opioid receptors. Therefore, this study focused on the binding of the kratom alkaloids with the  $\mu$ -opioid receptor.

To go about binding to the receptor, several steps had to occur. The first was selecting and preparing the ligands for binding. The next step involved choosing the receptor for study (the  $\mu$ -opioid receptor) and importing it into the Maestro software. Once in the software, the protein was prepared through the Protein Preparation Wizard to resolve any issues occurring within the protein structure. Next, a grid was generated within the protein to prepare the binding pocket of the receptor for accurate docking of the ligands. Lastly, the previously prepared ligands were docked within the receptor grid through the standard precision method, which produced a GlideScore and Glide Emodel score for each of the ligands. These scores helped determine the overall best pose for each ligand that would give the best binding to the receptor. Binding free energy estimations were also calculated for each ligand to determine a ranking of which ligands

have stronger affinity to the receptor. All of these values were used to compare the alkaloids to each other as well as to other opioids and opiates.

It was determined that all of the kratom alkaloids interact in some way with either HIS 54 or ASP 147 or, in the case of mitragynine, with both. These two residues are two of the essential residues needed for interaction with the  $\mu$ -opioid receptor. The alkaloids did not exhibit any salt-bridge or  $\pi$ - $\pi$  stacking interactions within the binding pocket unlike the opioids and opiates. The alkaloids also each exhibited similar numbers of residue interactions for the hydrophobic, polar, positively charged, and negatively charged residues. All of the alkaloids also contained the same 5 polar residues within their binding pockets: HIS 54, SER 55, ASN 127, GLN 124, and HIE 297. MM-GBSA values ranked similarly with binding affinities, with only two not fitting the pattern, 7-hydroxymitragynine and mitragynine pseudoindoxyl.

When comparing the alkaloids to the other chosen opioids and opiates, a few similarities and differences were seen between them. The first noticeable similarity is that every opioid and opiate ligand have salt-bridge and/or  $\pi$ - $\pi$  stacking interactions within the binding pocket. These interactions are not seen within the alkaloids. The salt-bridges are also with ASP 147 which the alkaloids, not all though, interact with through hydrogen bonding. Through  $\pi$ -cation interactions, the opioids and opiates interact with TYR 148, and the alkaloids interact with HIS 54. The only two ligands to interact with HIS 54 through hydrogen bonding are methadone and paynantheine. When comparing their number of residue interactions, the alkaloids, opioids, and opiates do not share similar numbers. The only two that share very close numbers to the alkaloids are carfentanil and fentanyl. Carfentanil, fentanyl, mitragynine, and 7-hydroxymitragynine all share the same

15 hydrophobic residues, 6 polar residues, and both of the positively and negatively charged residues. It was also notable that three of those four ligands, carfentanil, fentanyl, and mitragynine, shared a hydrogen bond with ASP 147 while 7-hydroxymitragynine did not. The ranking of these four using their MM-GBSA values was very similar to their binding affinity order.

During the docking of the ligands, buprenorphine began to pose a large issue. At first, the structure which was taken from the PubChem website would not dock at all, and multiple attempts to do so failed. This specific structure also gave a positive MM-GBSA value when it should be negative. To test for possible reasons of this positive value, the MM-GBSA value was calculated using different sampling methods: with and without constraints, with and without constraints on side chains, and with and without constraints on polar hydrogens. None of these were able to bring about a negative MM-GBSA value for buprenorphine. Therefore, the next step was to see if the structure of buprenorphine could be the possible issue. Several tests were done with both the 2D and 3D structures of buprenorphine downloaded from multiple sites. The only structure to give a negative MM-GBSA value was the two-dimensional structure from ChemSpider. One downloaded structure even gave a more positive value than the PubChem structure. To that end, it was decided that the possible reasons for the issue could be due to differing file types, having corrupted files, or difficulty in the software of handling a complicated structure.

While the study was a good starting point for the understanding of how kratom interacts with receptors in the body, there are still many important aspects that have yet to be covered. One future goal is to examine the distances of the specific interactions of the alkaloids,  $\pi$ -cation and hydrogen bonding, to see if these aspects influence the docking

scores and binding energies of the ligands. Each ligand interaction diagram was originally analyzed at 5 angstroms, so looking at the residue distance at 6 or 7 angstroms could provide more clues as to other specific interacting residues within the binding pocket. Because the structure of the compound is important to the binding of a ligand, drawing new structures based on the alkaloids would be beneficial to study to see if certain structural groups influence binding to the receptor as well. As each of the alkaloids exhibit some kind of interaction with two of the other opioid receptors, it would be important to see what kinds of interactions occur between the alkaloids and the  $\kappa$ - and  $\delta$ - opioid receptors as well. However, the overall goal of this project is to create a database that contains all relevant information of the kratom alkaloids, including their binding interactions as well as their analytical instrumentation data, and other psychoactive substances so as to make it easier for forensic chemists and other laboratory technicians to find vital information on these up and coming substances.

## **References:**

1. Hassan, Z., Muzaimi, M., Navaratnam, V., Yusoff, N. H. M., Suhaimi, F. W., Vadivelu, R., . . . Müller, C. P. (2013). From kratom to mitragynine and its derivatives: Physiological and behavioural effects related to use, abuse, and addiction. *Neuroscience and Biobehavioral Reviews*, 37(2), 138-151. doi:10.1016/j.neubiorev.2012.11.012
2. Meireles, V., Rosado, T., Barroso, M., Soares, S., Gonçalves, J., Luís, Â., . . . Gallardo, E. (2019). Mitragyna speciosa : Clinical, toxicological aspects and analysis in biological and non-biological samples. *Medicines (Basel, Switzerland)*, 6(1), 35. doi:10.3390/medicines6010035
3. Singh, D., Narayanan, S., & Vicknasingam, B. (2016). Traditional and non-traditional uses of mitragynine (kratom): A survey of the literature. *Brain Research Bulletin*, 126(Pt 1), 41-46. doi:10.1016/j.brainresbull.2016.05.004
4. Grundmann, O. (2017). Patterns of kratom use and health impact in the US—Results from an online survey. *Drug and Alcohol Dependence*, 176, 63-70. doi:10.1016/j.drugalcdep.2017.03.007
5. Kruegel, A. C., Gassaway, M. M., Kapoor, A., Váradi, A., Majumdar, S., Filizola, M., . . . Sames, D. (2016). Synthetic and receptor signaling explorations of the mitragyna alkaloids: Mitragynine as an atypical molecular framework for opioid receptor modulators. *Journal of the American Chemical Society*, 138(21), 6754-6764. doi:10.1021/jacs.6b00360
6. Takayama, H., Ishikawa, H., Kurihara, M., Kitajima, M., Aimi, N., Ponglux, D., . . . Horie, S. (2002). Studies on the synthesis and opioid agonistic activities of

- mitragynine-related indole alkaloids: Discovery of opioid agonists structurally different from other opioid ligands. *Journal of Medicinal Chemistry*, 45(9), 1949-1956. doi:10.1021/jm010576e
7. Kruegel, A. C., & Grundmann, O. (2018). The medicinal chemistry and neuropharmacology of kratom: A preliminary discussion of a promising medicinal plant and analysis of its potential for abuse. *Neuropharmacology*, 134(Pt A), 108-120. doi:10.1016/j.neuropharm.2017.08.026
  8. Notes from the Field: Kratom (*Mitragyna speciosa*) Exposures Reported to Poison Centers - United States, 2010–2015 | MMWR. (2016, July 29). Retrieved from <https://www.cdc.gov/mmwr/volumes/65/wr/mm6529a4.htm#suggestedcitation>
  9. Docking and Scoring. (n.d.). Retrieved from <https://www.schrodinger.com/science-articles/docking-and-scoring>
  10. Notes from the Field: Unintentional Drug Overdose Deaths with Kratom Detected - 27 States, July 2016–December 2017 | MMWR. (2019, April 12). Retrieved from <https://www.cdc.gov/mmwr/volumes/68/wr/mm6814a2.htm>
  11. Maestro, Schrödinger, LLC, New York, NY, 2015.
  12. Huang, W., Manglik, A., Venkatakrishnan, A. J., Laeremans, T., Feinberg, E. N., Sanborn, A. L., . . . Kobilka, B. K. (2015). Structural insights into [mu]-opioid receptor activation. *Nature*, 524(7565), 315. doi:10.1038/nature14886
  13. PubChem. (n.d.). Retrieved from <https://pubchem.ncbi.nlm.nih.gov/>
  14. Váradi, A., Marrone, G. F., Palmer, T. C., Narayan, A., Szabó, M. R., Le Rouzic, V., . . . Majumdar, S. (2016). Mitragynine/Corynantheidine pseudoindoxyls as

- opioid analgesics with mu agonism and delta antagonism, which do not recruit  $\beta$ -arrestin-2. *Journal of Medicinal Chemistry*, 59(18), 8381-8397.  
doi:10.1021/acs.jmedchem.6b00748
15. Ellis, C. R., Kruhlak, N. L., Kim, M. T., Hawkins, E. G., & Stavitskaya, L. (2018). Predicting opioid receptor binding affinity of pharmacologically unclassified designer substances using molecular docking. *Plos One*, 13(5), e0197734. doi:10.1371/journal.pone.0197734
16. *Tramadol: Update Review Report*[PDF]. (2014, June). World Health Organization.
17. (n.d.). Retrieved from  
<http://www.guidetopharmacology.org/GRAC/RefineChemicalStructureSearchForward?ligandId=1670>

## APPENDIX

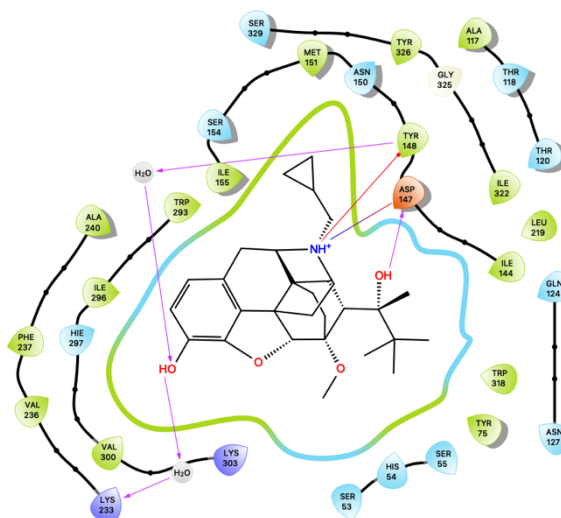


Figure A-1: Ligand-receptor interaction diagram for buprenorphine

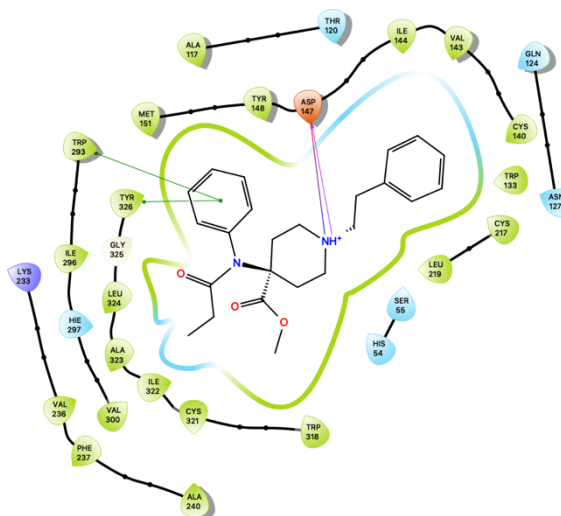


Figure A-2: Ligand-receptor interaction diagram for carfentanyl



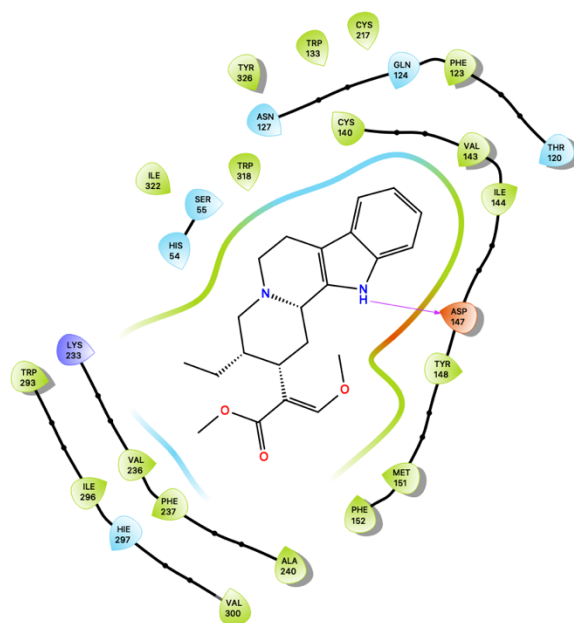


Figure A-3: Ligand-receptor interaction diagram for corynantheidine

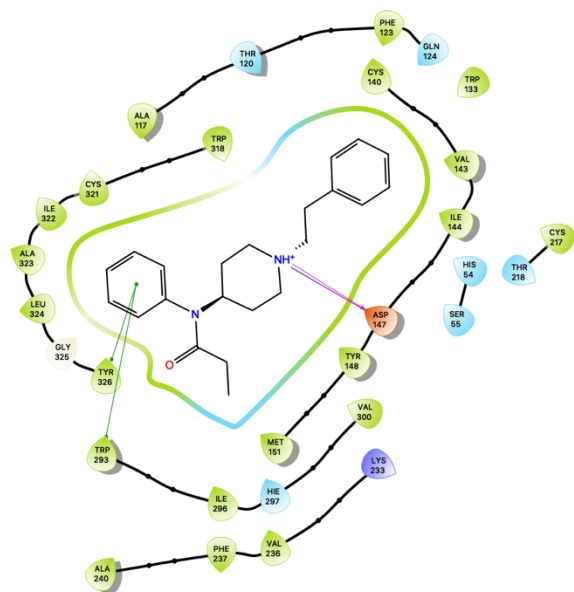


Figure A-4: Ligand-receptor interaction diagram for fentanyl

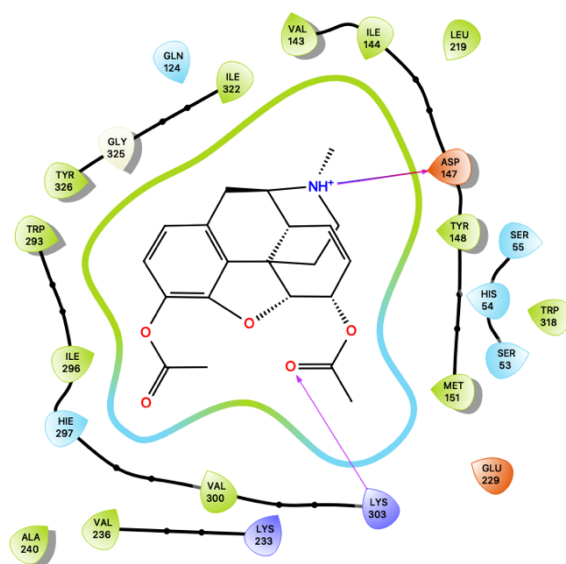


Figure A-5: Ligand-receptor interaction diagram for heroin

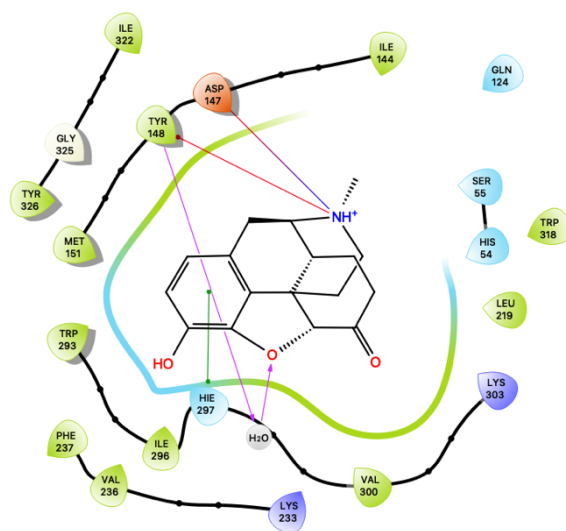


Figure A-6: Ligand-receptor interaction diagram for hydromorphone

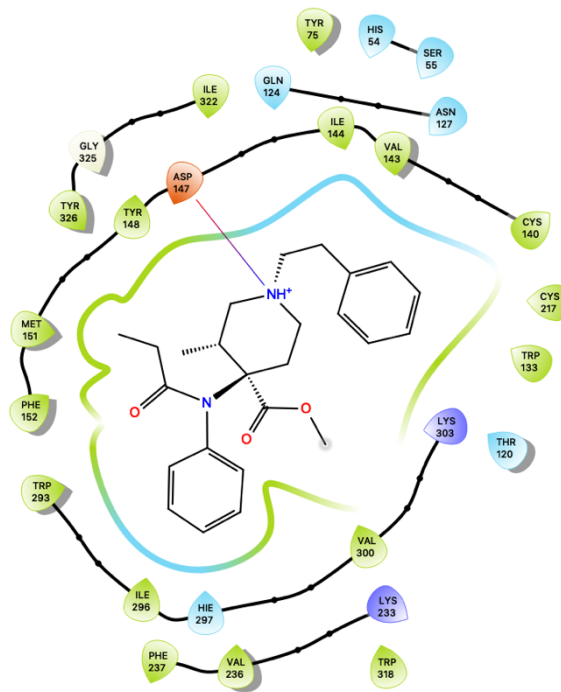


Figure A-7: Ligand-receptor interaction diagram for lofentanyl

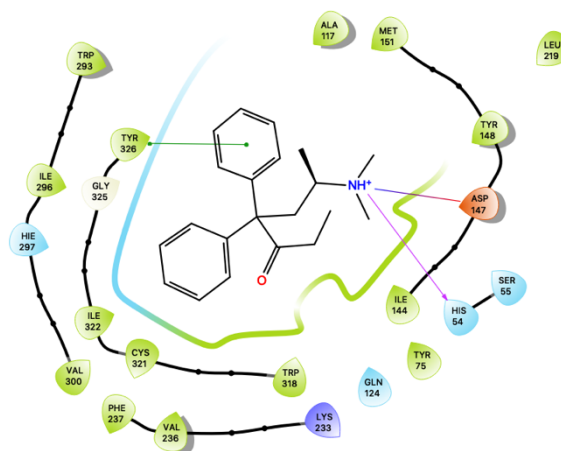


Figure A-8: Ligand-receptor interaction diagram for methadone

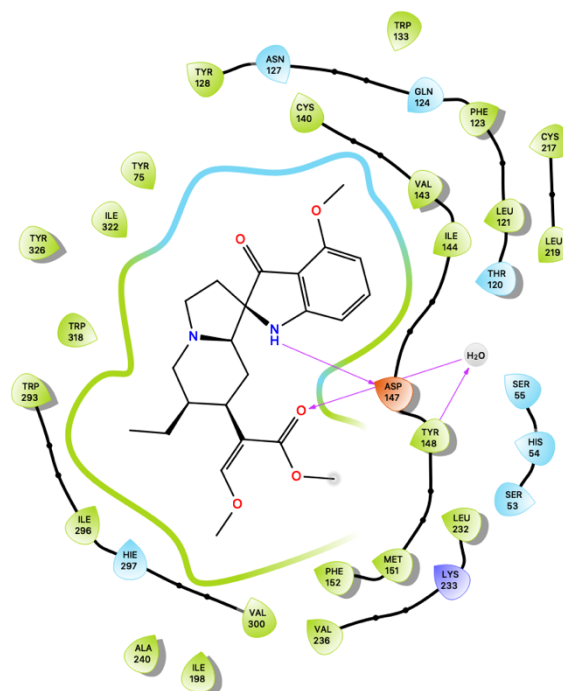


Figure A-9: Ligand-receptor interaction diagram for mitragynine pseudoindoxyl

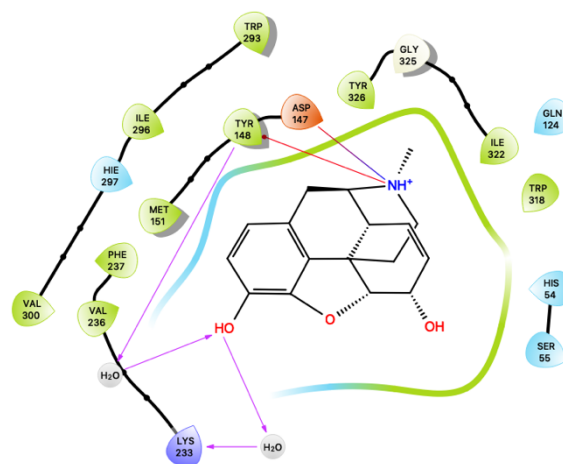


Figure A-10: Ligand-receptor interaction diagram for morphine

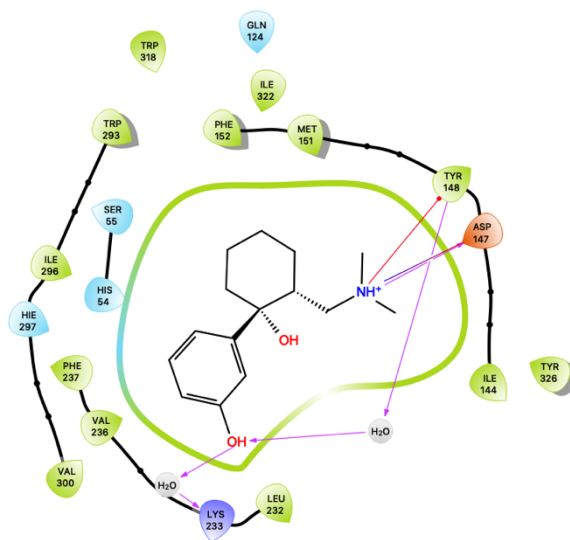


Figure A-11: Ligand-receptor interaction diagram for o-desmethylnaltrexone

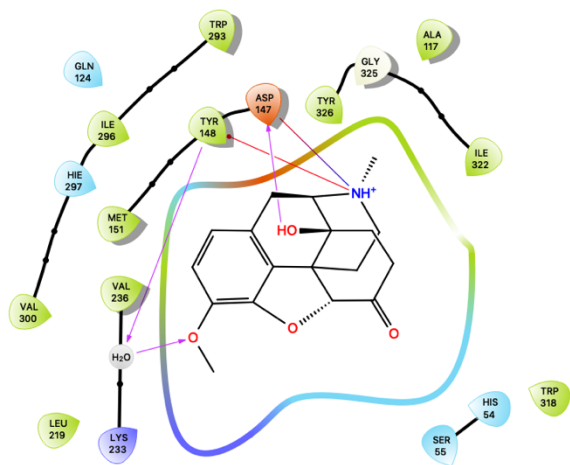


Figure A-12: Ligand-receptor interaction diagram for oxycodone

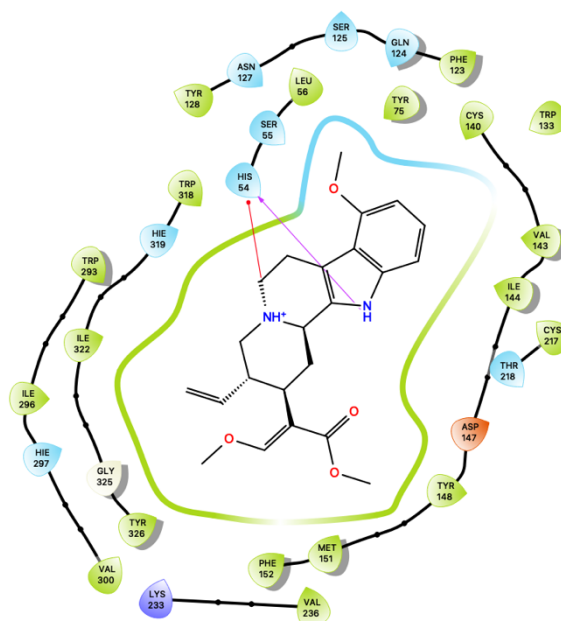


Figure A-13: Ligand-receptor interaction diagram for paynantheine

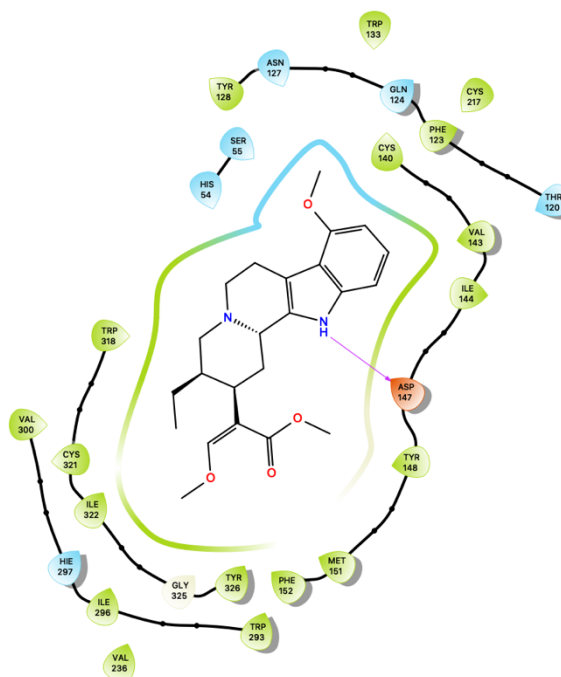


Figure A-14: Ligand-receptor interaction diagram for speciociliatine

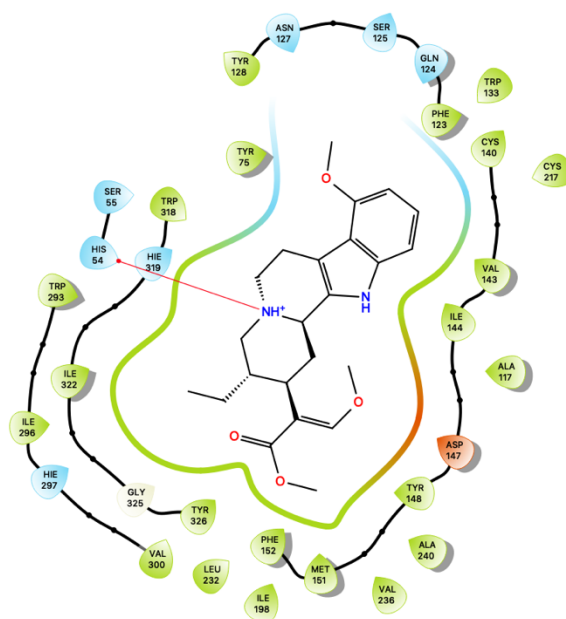


Figure A-15: Ligand-receptor interaction diagram for speciogynine

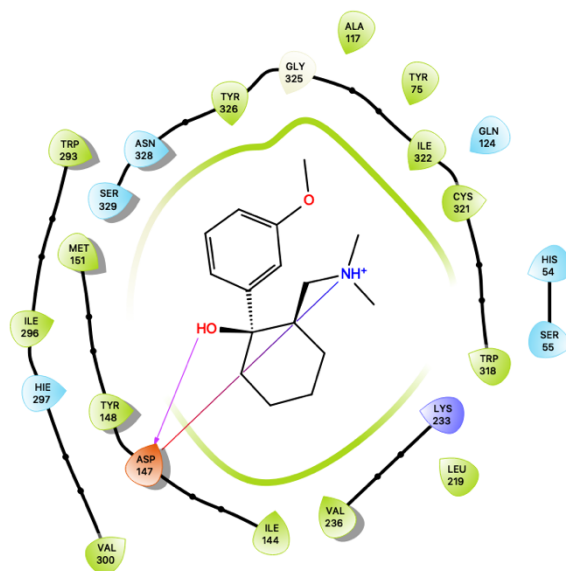


Figure A-16: Ligand-receptor interaction diagram for tramadol